



HAL
open science

Active suppression of temperature oscillation from a pulse-tube cryocooler in a cryogen-free cryostat: Part 1. Simulation modeling from thermal response characteristics

Changzhao Pan, Bo Gao, Yaonan Song, Haiyang Zhang, Dongxu Han, Jiangfeng Hu, Wenjing Liu, Hui Chen, Mark Plimmer, Fernando Sparasci, et al.

► To cite this version:

Changzhao Pan, Bo Gao, Yaonan Song, Haiyang Zhang, Dongxu Han, et al.. Active suppression of temperature oscillation from a pulse-tube cryocooler in a cryogen-free cryostat: Part 1. Simulation modeling from thermal response characteristics. *Cryogenics*, 2020, 109, pp.103097. 10.1016/j.cryogenics.2020.103097 . hal-04032211

HAL Id: hal-04032211

<https://hal.science/hal-04032211>

Submitted on 16 Mar 2023

HAL is a multi-disciplinary open access archive for the deposit and dissemination of scientific research documents, whether they are published or not. The documents may come from teaching and research institutions in France or abroad, or from public or private research centers.

L'archive ouverte pluridisciplinaire **HAL**, est destinée au dépôt et à la diffusion de documents scientifiques de niveau recherche, publiés ou non, émanant des établissements d'enseignement et de recherche français ou étrangers, des laboratoires publics ou privés.

1 **Active suppression of temperature oscillation from a pulse-tube cryocooler**
2 **in a cryogen-free cryostat: Part 1. Simulation modeling from thermal**
3 **response characteristics**

4 Changzhao Pan^{1,2, a)}, Bo Gao^{1,3,4, a)}*, Yaonan Song^{1,3, 5}, Haiyang Zhang^{1,3}, Dongxu Han⁵,
5 Jiangfeng Hu^{1,3,4}, Wenjing Liu^{1,3,5}, Hui Chen^{1,3,6}, Mark Plimmer^{1,2}, Fernando Sparasci^{1, 2},
6 Ercang Luo^{1,3,4}, Laurent Pitre^{1,2}

7 ¹ *TIPC-LNE Joint Laboratory on Cryogenic Metrology Science and Technology, Chinese Academy of Sciences*
8 *(CAS), Beijing 100190, China*

9 ² *LCM-LNE-Cnam, 61 rue du Landy, 93210 La Plaine-Saint Denis, France*

10 ³ *Key Laboratory of Cryogenics, Technical Institute of Physics and Chemistry, Chinese Academy of Sciences,*
11 *Beijing, 100190, China*

12 ⁴ *University of Chinese Academy of Sciences, Beijing 100490, China*

13 ⁵ *Beijing Institute of Petrochemical Technology, Beijing 102617, China*

14 ⁶ *Xi'an Jiaotong University, Xian 710049, China*

15 **Abstract:**

16 A cryogen-free cryostat cooled using a 4 K commercial GM or pulse tube cryocooler (PTC) displays
17 temperature oscillations caused by the intrinsic working principle of the regenerative cryocooler. To
18 dampen such oscillations usually requires either a large heat capacity or a large thermal resistance. To
19 understand this phenomenon better and suppress it more effectively, both the step response
20 characteristic and the intrinsic oscillation characteristic of cryostat have been used to obtain the
21 complete transfer functions of a simulation model. The latter is used to test and optimize traditional
22 PID feedback control. The results showed this approach has almost no effect on the temperature
23 oscillation amplitude. Based on this simulation model, a novel active method was proposed and tested
24 numerically. Simulation results predict the method should suppress the amplitude of the original
25 temperature oscillation by a factor of two.

26 **Keywords:** Pulse tube cryocooler, Cryogen-free cryostat, Thermal response characteristics, Transfer function
27 method, active control

28
29
30
31 * Author to whom correspondence should be addressed. Email: bgao@mail.ipc.ac.cn;

32 a) These authors contributed to the work equally and should be regarded as co-first authors

1 **Nomenclature**

2 A, B Temperature amplitudes (K)

3 C Heat Capacity ($\text{J}\cdot\text{kg}^{-1}\cdot\text{K}^{-1}$)

4 $G(s)$ Transfer function

5 $L(s)$ Laplace transform

6 M Mass (kg)

7 Q Heat (W)

8 R Thermal Resistance ($\text{K}\cdot\text{W}^{-1}$)

9 t Time (s)

10 T Temperature (K)

11

12 Greek letters

13 α, θ Phase angle (rad)

14 ω Angular frequency ($\text{rad}\cdot\text{s}^{-1}$)

15 τ Time constant (s)

16

17

18

19

20

21

22

23

1 **1. Introduction**

2 Primary gas thermometry (PGT) methods, such as constant-volume gas thermometry
3 (CVGT) [1], dielectric-constant gas thermometry (DCGT) [2], acoustic gas thermometry
4 (AGT) [3] and single-pressure refractive-index gas thermometry (SPRIGT) [4], measure
5 thermodynamic temperature with the highest accuracy. The related instruments need to
6 measure the pressure or some other parameters of the working gas (dielectric constant, speed
7 of sound *etc.*) at a stable temperature for one to obtain the thermodynamic temperature. For
8 example, SPRIGT has the potential to yield an uncertainty of 0.25 mK in the range 5 K to
9 25 K via the measurement of a resonant microwave frequency. However, it also requires a
10 very high temperature stability working environment with a standard uncertainty below
11 0.2 mK. More generally, a cryostat with ultra-high temperature stability is essential for all
12 types of PGT.

13 Cryostats working at temperatures well below 77 K such as those used in DCGT [2] and
14 AGT [3] often use liquid helium as the refrigerant. However, the need to refill them with
15 helium results in the experiment being discontinuous while the changing liquid gives rises to
16 constantly evolving operating conditions. Moreover, the boiling of liquid helium adds a large
17 thermal noise to the experimental system, especially in the temperature range above 25 K,
18 which makes stable operation of the cryostat difficult [3]. In recent years closed-cycle
19 cryocoolers such as the commercial 4K Gifford-McMahon (GM) cryocooler or the GM-type
20 pulse tube cryocooler (GM-PTC) have been used as an alternative. Cryostats cooled this way,
21 also called cryogen-free cryostats, can be compact and run uninterrupted for several months
22 or even years. They can be used from room temperature down to around 3 K. Naturally, they
23 have attracted increasing interest [5] [6] [7].

24 At low temperatures (especially below 77 K), however, systems cooled by both the 4K
25 GM cryocooler and the GM-PTC show temperature oscillations caused by the periodic
26 compression and expansion within the cryocooler. At temperatures below 20 K, because of
27 the low heat-capacity of the material within the cryostat, this oscillation becomes even more
28 manifest, thereby hindering temperature regulation.

29 Thus far, two main approaches have been employed to attenuate this oscillation, namely,
30 the heat-capacity method (HCM) and the thermal-resistance method (TRM). The HCM uses a
31 material of large heat-capacity at low temperature, such as a pressurized helium pot, lead, or a
32 rare-earth alloy (such as ErNi and Er₃Ni). Li *et al.* [8], Okidono *et al.* [9] and Webber *et al.*
33 [10] attached a helium filled pot onto the cold end of a GM cryocooler, thereby reducing the

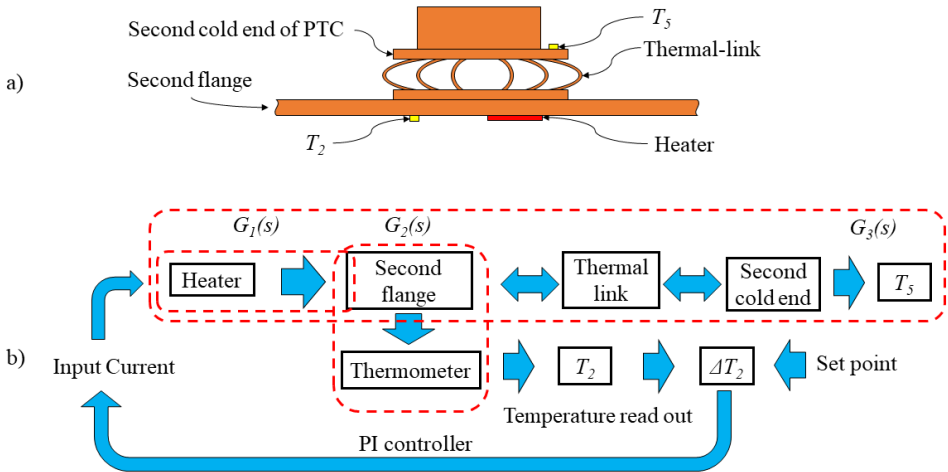
1 peak-to-peak temperature oscillation at 4 K from a few hundred millikelvin to below 50 mK.
2 Fluhr *et al.* and [11], Huang *et al.* [12] used a lead plate to reduce the oscillation amplitude to
3 the millikelvin level. Allweins *et al.* [13] and Shen *et al.* [14] used ErNi alloy with a GM-PTC
4 and attenuated the amplitude to around 10 mK at 4 K. However, while the HCM can suppress
5 the oscillation with almost no increase in lowest working temperature, the additional heat
6 capacity it adds significantly increases the cooling time (typically by an order of magnitude).

7 The other approach, the TRM, uses a material with low thermal-conductivity at low
8 temperature. Using a fibre-reinforced-plastic (FRP) damper, Nakamura *et al.* [15] reduced the
9 oscillation amplitude at 4.2 K to 0.7 mK while Dong *et al.* [16] using a
10 polytetrafluoroethylene (PTFE) sheet, brought the thermal oscillation amplitude at 20 K down
11 to below 4 mK. Finally, Dubuis *et al.* [17], using lead plates with stainless steel spacers to
12 combine both methods, obtained a temperature stability better than 1 mK. While the TRM
13 does not increase the cooling time, it does cause a temperature jump between the cryocooler
14 and the flange it cools, which leads to a loss of cooling power (by as much as several watts,
15 depending on the thermal resistance).

16 In addition to the two methods above, in our previous experiment [18] [19] [20], a heat-
17 switch was used to attenuate the temperature modulation.

18 All the aforementioned techniques, while effective, are passive, their performance
19 depending on the structure of the cryostat. Moreover, their performance cannot be modified
20 during the course of the experiment. For this reason, we have sought instead to use active
21 temperature stabilisation. The most commonly used active method is Proportional-Integral
22 (PI) control. To optimise regulation, researchers have developed many theories on tuning PI
23 coefficients [21] [22]. Even so, the study of feedback control with thermal oscillation is rare.
24 Bhatt *et al.* [23] used the transfer function of a cryocooler to help tune the PI control
25 coefficients of their system. To model the thermal behavior of their cryocooler, Sosso *et al.*
26 [24] used linear system theory, which can be effective in the design of temperature controllers.
27 Nevertheless, both these groups' research was only focused on the cold end of the cryocooler
28 itself, and not the cryostat it was cooling. Complete mastery of active control requires that one
29 develop a model for the entire system. Only then can one expect to obtain optimal suppression
30 of temperature oscillation in a cryogen-free cryostat. In the present work, such a model was
31 developed and implemented. It allowed the thermal characteristics of the system to be
32 deduced by experiment. Moreover, it highlighted the inefficacy of traditional PI control and
33 led us to invent a different method for removing thermal oscillations more effectively (by a
34 factor of two).

1 The remainder of the paper is structured as follows. First, the cryostat and cooler are
 2 briefly described. The simulation model is presented, followed by the results obtained when it
 3 was implemented with the experiment allowing the determination of all the thermal transfer
 4 functions. Finally, the novel active suppression method is described.



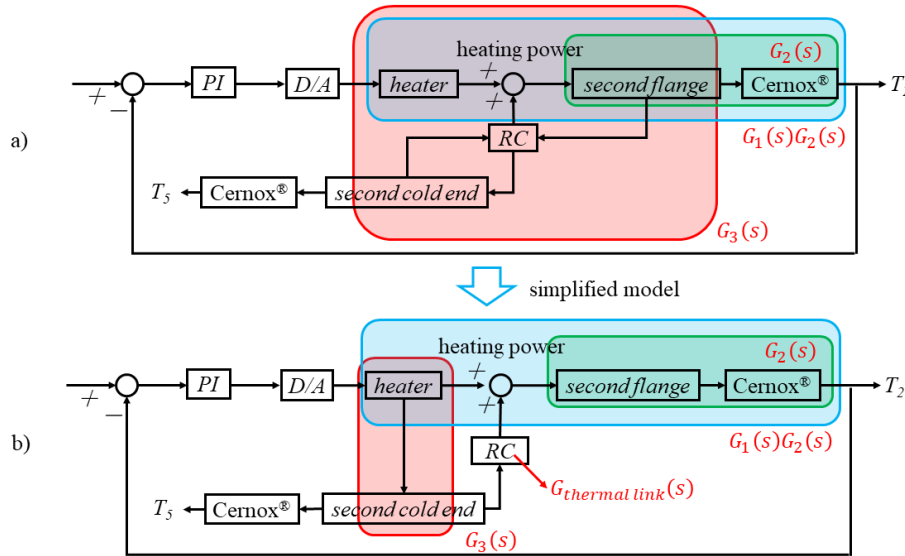
5
 6 Figure 1. a). Schematic diagram of the experimental system b). Schematic diagram of the PI
 7 temperature control feedback loop. PTC: Pulse-Tube Cryocooler. The labels T_2 and T_5 refer to
 8 two of the many thermometers placed throughout the system [18], [19].

9 **2. Cryogenic apparatus**

10 The cryostat studied in this paper was that used in our system for SPRIGT, a detailed
 11 description of which can be found in references [18] [19] and [20]. It was cooled by a
 12 commercial Sumitomo GM-type pulse tube cryocooler (PTC), which can yield a lowest
 13 temperature of 2.8 K, and can supply 1 W cooling power at 4.2 K. Figure 1 shows the
 14 structural diagram of the main components studied in this work. A flexible thermal-link was
 15 used to connect the second cold end of PTC and the second flange. The heat capacity of the
 16 flange and the contact resistances of the thermal link provide passive damping of the
 17 oscillation from the PTC. Despite this, the temperature of the second flange still exhibits an
 18 oscillation with a peak-to-peak amplitude of several millikelvin. Moreover, these thermal
 19 oscillations can diffuse into the pressure tube and pressure vessel and thereby degrade the
 20 stability of *pressure* regulation too¹. To regulate the temperature of the second flange, a heater

¹ The microwave resonator for SPRIGT is housed within a pressure vessel, the latter connected to a pressure control system at room temperature via a long tube. Wherever this tube passes through a flange, a thermal-link

1 and two calibrated thermometers (Lakeshore Cernox model CX1050-CU-HT-1.4L²) were
 2 used.



3
 4 Figure 2 a). Actual temperature control system b). Simplified representation used to model it.

5 3. Simulation model

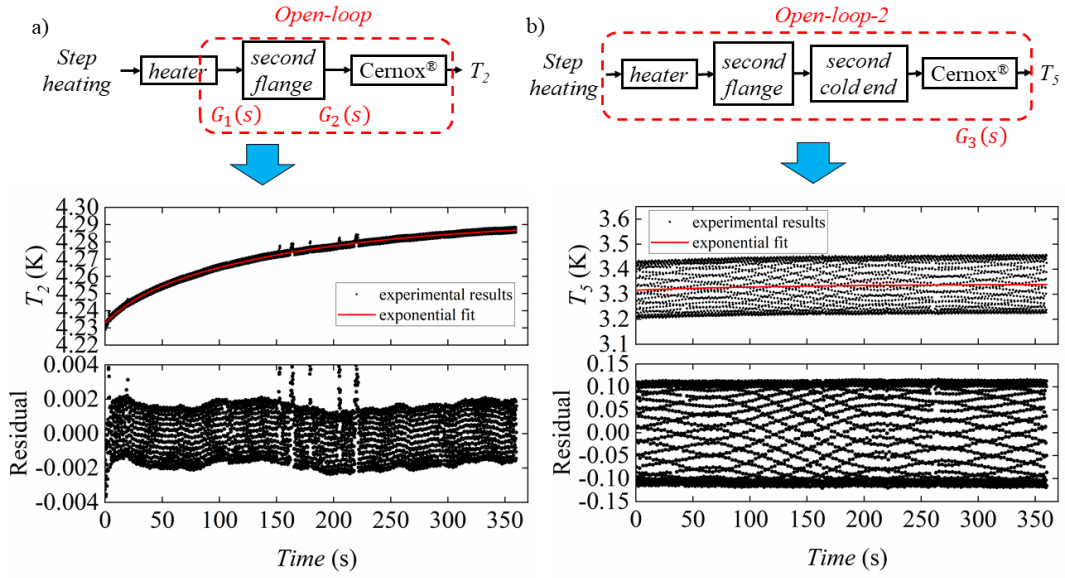
6 A schematic of the real temperature control system is shown in figure 2(a). To regulate
 7 the temperature of the cryostat better and reduce this oscillation, a simplified temperature
 8 control system block diagram was developed (Figure 2(b)). Two factors influence the
 9 temperature of the flange: the cooling power from the second cold end of the PTC and the
 10 heat supplied by the heater. However, the heater also warms the second cold end of the PTC.
 11 To simplify the simulation model, the heat transfer paths are reduced to four modules
 12 (figure 2b). The first module concerns the heat transfer from the heater to the flange, modelled
 13 by the function $G_1(s)$. The second module involves the heat transfer from the flange to the
 14 thermometer, modelled by the function $G_2(s)$. The third, modelled by the function $G_3(s)$,
 15 quantifies the heat transfer from the heater to the second cold end of the PTC and then to
 16 another thermometer. Finally, the effect of the thermal link is modelled by the transfer
 17 function $G_{thermal\ link}(s)$.

was added to reduce its temperature. So any temperature oscillation on the flange would be transferred to the pressure tube, thereby causing the pressure to oscillate and degrading the stability of pressure regulation.

²To simplify the installation of the thermometer, the CU type package was used in the experiment. But the relatively low thermal response time of the CX1050-CU sensor partially attenuated the amplitude of the temperature oscillation. From a relative standpoint, this had no influence on the outcome of the research. However, we suggest the reader use preferably a thermometer with a faster response to measure the dynamic temperature, such as the models CX1050-SD, BC or similar.

1 These four transfer functions are enough to describe the main thermal response
 2 characteristics. To obtain expressions for them, a step response experiment was performed on
 3 the flange and the second cold end of the PTC. As shown in figure 3, a heat step (from 0 to
 4 8.8 mW) was added by the heater to the open loop system. The transfer functions $G_1(s)$ and
 5 $G_3(s)$ were then obtained by using the ratio of the Laplace transform of the output function to
 6 the Laplace transform of the excitation step heating function. Indeed, according to references
 7 [22] and [24], the best fit of the temperature response to a power step input can be accurately
 8 described by a sum of exponential decays:

$$9 \quad T(t) = A_0 + A_1(1 - e^{-t/\tau_1}) + A_2(1 - e^{-t/\tau_2}) + \dots \quad (1)$$



10
 11 Figure 3. Step responses of a) the flange and b) the PTC second cold end temperatures, T_2 and
 12 T_5 respectively.

13 Table 1. The fitted functions of the stepwise heating and intrinsic sinusoidal response.

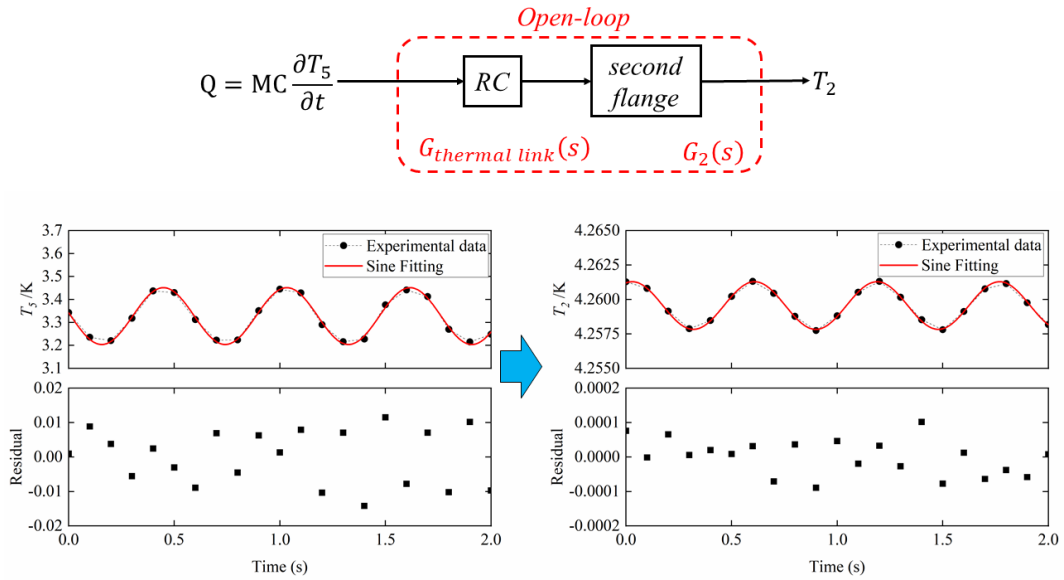
		Fitted function
Step response	T_2 (K)	$4.23 + 0.01(1 - e^{-t/26.48}) + 0.05(1 - e^{-t/165.41})$
	T_5 (K)	$3.34 - 0.024(1 - e^{-t/134.96})$
Sinusoidal response	T_2 (K)	$4.26 + 0.0017 \times \sin(10.84t + 1.89)$
	T_5 (K)	$3.33 + 0.12 \times \sin(10.76t + 3.02)$

14

1 To simplify the model, a first-order response function was used to describe heat
 2 transfer from the heater to the second-stage cold end of the PTC. A second-order response
 3 function was used to describe that from the flange to thermometer, because it contains two
 4 parts $G_1(s)$ and $G_2(s)$ and has two time-constants. Figures 3 a) and b) show the response
 5 curves of the flange and the second-stage cold end of the PTC. The fitted response functions
 6 can be found in table 1. From its Laplace transform, we obtain the following expressions for
 7 the transfer functions:

$$8 \quad G_1(s)G_2(s) = \frac{340.91s+6.82}{(26.48s+1)(165.41s+1)} \quad (2)$$

$$9 \quad G_3(s) = \frac{2.77}{135s+1} \quad (3)$$



10

11 Figure 4 The sinusoidal response from the PTC to the thermometer on the second flange.

12 In addition to the step response method, the sinusoidal response method can also be
 13 used to obtain information on the transfer functions. In the present system, there always exists
 14 a temperature oscillation propagating from the second cold end of PTC to flange³. This means
 15 there also exists a heat oscillation (around a mean value of zero) travelling between the
 16 second-stage cold end of the PTC and the flange. Thus, by analyzing this intrinsic sinusoidal
 17 response, one can obtain an expression for transfer function. As shown in figure 4, this heat
 18 oscillation can be expressed by the derivative of T_5 , propagating through the thermal link and

³ For the GM type cryocooler, the pressure wave inside of cryocooler is not actually a sine wave, but rather more like a square wave (containing the fundamental and odd harmonics), so the temperature oscillation of the working gas should be non-sinusoidal. However, because of the heat capacity of the cold end, the higher-order harmonics are greatly filtered, resulting in the measured temperature being essentially sinusoidal after all.

1 the second flange to the thermometer T_2 . By applying the Laplace transform to this open loop
 2 response, one can obtain the complete transfer function from the second cold end of the PTC
 3 to the thermometer on the second flange:

$$4 \quad G_{thermal-link}(s) \cdot G_2(s) = \frac{L(T_2 - A_0)}{L(Q)} = \frac{1}{MC} \frac{\frac{A_1 \sin \theta}{-\omega^2 B_1 \sin \alpha} s + \frac{A_1 \cos \theta}{-\omega B_1 \sin \alpha}}{\frac{\cos \alpha}{-\omega \sin \alpha} s + 1} \quad (4)$$

5 Here, the transfer function of the thermal link $G_{thermal-link}(s)$ can be expressed in terms
 6 of its time constant RC :

$$7 \quad G_{thermal-link}(s) = \frac{F_{thermal-link}(s)}{RCs + 1} \quad (5)$$

8 while the transfer function $G_2(s)$ can be written as:

$$9 \quad G_2(s) = \frac{F_2(s)}{\tau_2 s + 1} \quad (6)$$

10 In our previous work, the thermal resistance of the thermal-link was calculated
 11 accurately [19]. At this temperature, $RC \approx 100$ ms, so the term RCs can be neglected to begin
 12 with in the actual calculation. Then, from equation of (4) (5) (6), we obtain:

$$13 \quad G_{thermal-link}(s) \cdot G_2(s) = \frac{1}{MC} \frac{\frac{A_1 \sin \theta}{-\omega^2 B_1 \sin \alpha} s + \frac{A_1 \cos \theta}{-\omega B_1 \sin \alpha}}{\frac{\cos \alpha}{-\omega \sin \alpha} s + 1} \approx \frac{F_{thermal-link}(s) \cdot F_2(s)}{\tau_2 s + 1} \quad (7)$$

14 On the other hand, there are two time-delays in the product of equation (2), which
 15 correspond the time constants of $G_1(s)$ and $G_2(s)$, respectively τ_1 and τ_2 . Because $G_2(s)$ is the
 16 transfer function describing heat flow from the flange to the thermometer, it should have the
 17 smaller time constant. Thus, we take $\tau_2 = 26.48$ s. To solve equation (7), one also needs to
 18 know the phase relationship between α and θ , which can be obtained by measuring T_2 and T_5
 19 simultaneously. In the experiment, a trigger device was used to control two Keithley 2002
 20 digital multimeters (DMM) to measure both temperatures at the same time. The phase
 21 difference $\alpha - \theta$ was found to be 1.134 rad, as shown in table 1.

22 When the following values of the other parameters are inserted, $M = 1.6$ kg, $A_1 =$
 23 0.00173 K, $B_1 = 0.12361$ K, $\omega = 10.83$ rad s^{-1} , equation (7) simplifies to:

$$24 \quad G_{thermal-link}(s) \cdot G_2(s) = \frac{-0.294s + 1.4732}{(0.15s + 1)(26.48s + 1)} \quad (8)$$

25 Comparing equations (2) and (8), the simplest solutions are:

$$G_1(s) = \frac{340.91s+6.82}{165.41s+1} \quad (9)$$

$$G_2(s) = \frac{1}{26.48s+1} \quad (10)$$

$$G_{thermal-link}(s) = \frac{-0.294s+1.4732}{0.1s+1} \quad (11)$$

4. Discussion

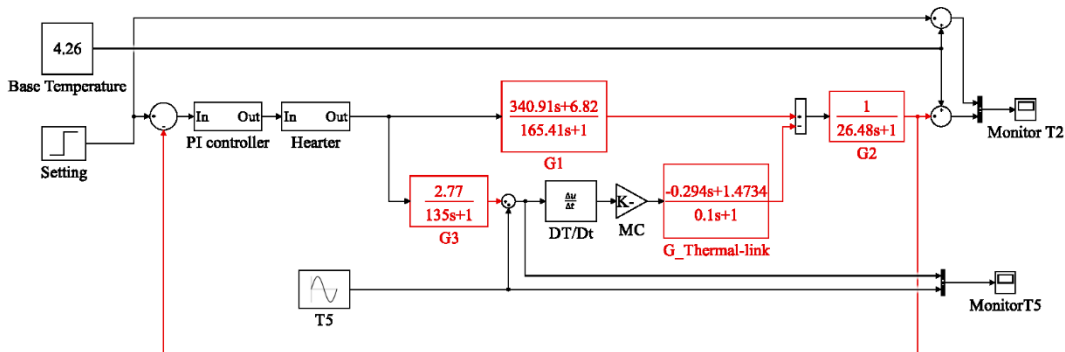
In this section, we describe the simulation model developed using MATLAB Simulink software and how simulation results were verified by experiment. Thereafter, we present a novel active suppression method to attenuate the thermal modulation intrinsic to cryogen-free cryostats.

9

4.1 Simulation results and verification

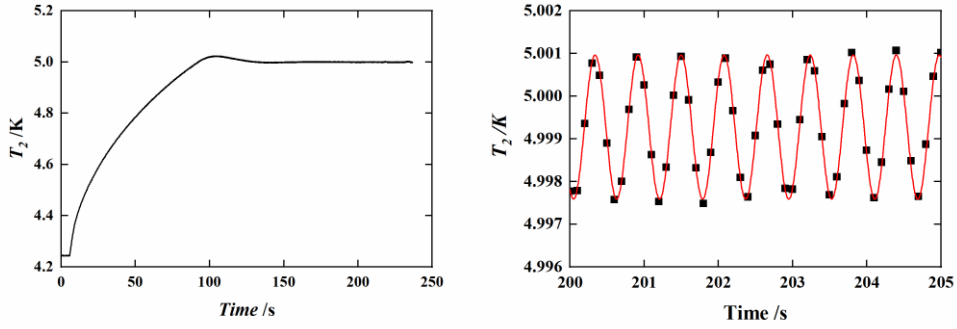
Based on above transfer functions, a simulation model for temperature regulation was developed using MATLAB Simulink software. As shown in figure 5, the heat on the flange can be split into two parts. The first is the heat from the heater, calculated using the transfer function $G_1(s)$. The second is the heat due to the temperature oscillation of the PTC, which can be calculated using the transfer function $G_{thermal-link}(s)$. Both heat sources warm the flange and so influence the thermometer temperature T_5 via the transfer function $G_2(s)$. In the simulation, the set point was controlled by a step signal, and the temperature evolution observed on a computer monitor.

19



20

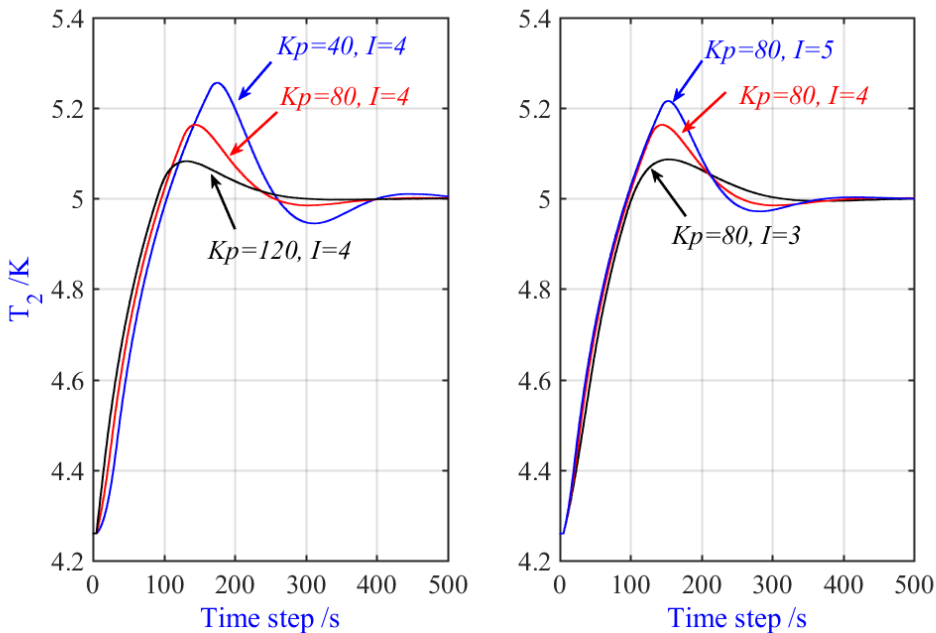
Figure 5 Simulation model written in MATLAB Simulink software



1

2 Figure 6. Experimental results for PI regulation of the second flange temperature T_2 . a)
 3 Temperature variation for the first 250 s. After 200 s, the mean value varies by less than 1 mK
 4 b). Oscillations around the set point

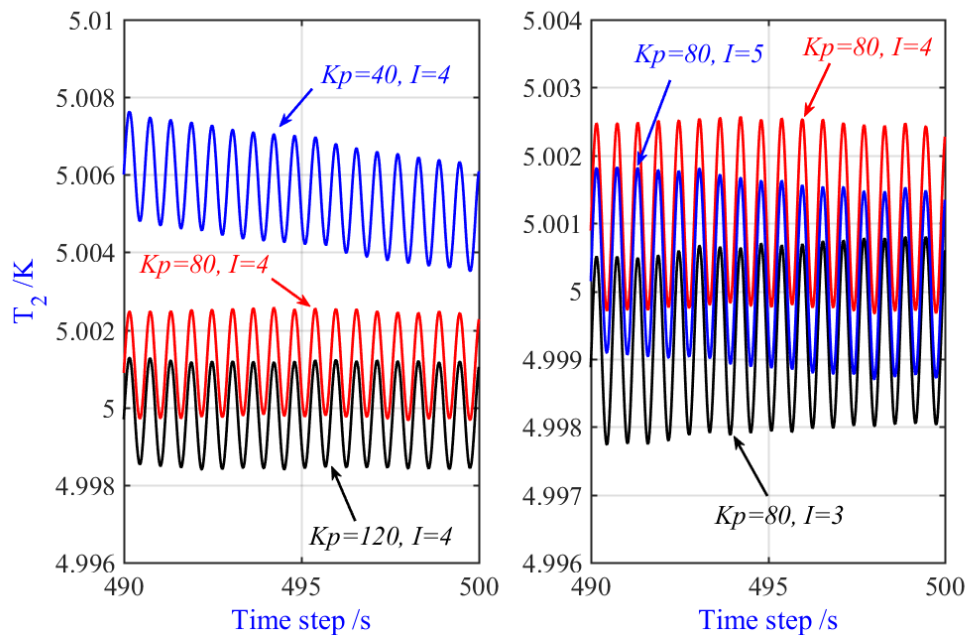
5 Figure 6 shows experimental results for temperature regulation at 5 K. In the
 6 experiment, the PI method was used to regulate the temperature on the flange, with $K_p = 80$,
 7 $I = 4$ and a sampling time of 80 ms. To avoid damage to the heater, the input current to the
 8 heater was limited to 100 mA. The results show it took about 150 s for the temperature T_5 to
 9 increase from 4.23 K to 5.00 K. In the steady state, T_2 still shows an oscillation with an
 10 amplitude around 1.5 mK.



11

12 Figure 7. Simulation results with different PI parameters (proportional gain K_p and integral
 13 gain I) showing temperature evolution towards equilibrium.

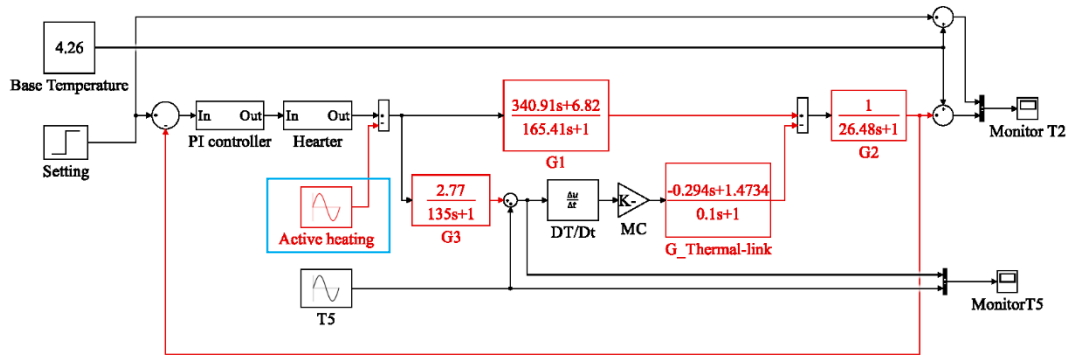
1 Figures 7 and 8 show the results obtained using the present simulation model. One
 2 observes that the overshoot value and stable time changed with different PI parameters.
 3 Because the maximum current was set at 100 mA in the simulation, a larger proportional gain
 4 K_p made the temperature reach its stable state more quickly and with a smaller overshoot
 5 value. By contrast, a larger integral coefficient I caused a larger overshoot value but had little
 6 effect on the stabilisation time. On the other hand, the PI parameters have almost no effect on
 7 the temperature oscillation amplitude (the amplitude of temperature oscillation changed by
 8 only 2% at most), which means the oscillation cannot be actively suppressed using traditional
 9 PI feedback. If in the simulation, temperatures appear to take a little longer to reach steady
 10 state than in the experiment, the final temperature oscillation amplitudes match experimental
 11 results well. The difference in stabilisation time might be caused by the changing of thermal
 12 diffusivity with temperature. Because the transfer function method is a 1D simulation, it is
 13 assumed that the whole system has a uniform temperature. However, in the real 3D
 14 experiment, the flange temperature shows some spatial variation. When the temperature
 15 changes from one value to another, even if the temperature of thermometer (located near the
 16 heater) has changed to that of the set point, it probably takes longer for the temperature to
 17 vary at a more distant location. Consequently, the experimental temperatures reach stability
 18 more quickly.



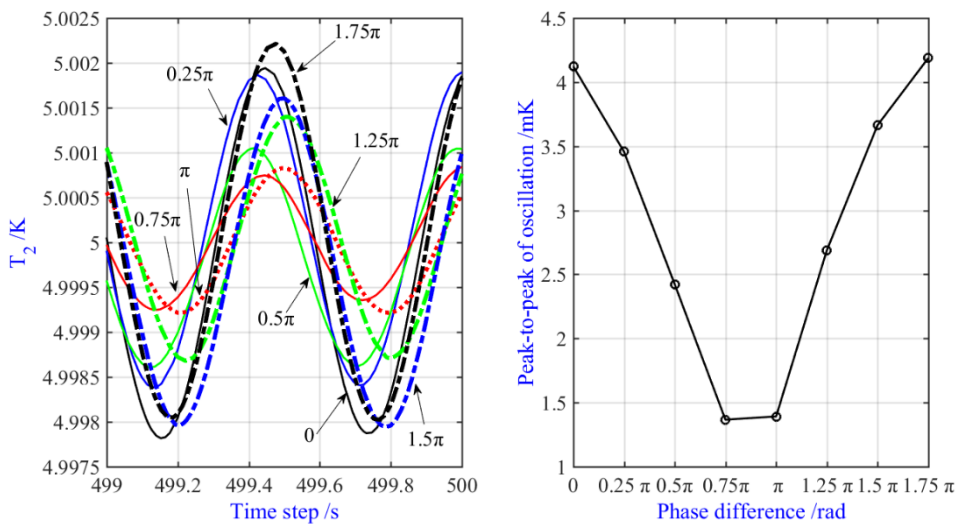
19

20 Figure 8. Simulation results with different PI parameters: temperature oscillations around the
 21 set point.

1 4.2 Active suppression method



2
3 Figure 9 The program used to model active suppression temperature oscillation method.



4
5
6 Figure 10 Simulation results for active suppression for eight different phase angles from 0 to
7 $7\pi/4$. The oscillation amplitude is minimized for a phase of between $3\pi/4$ and π .

8 Because traditional PI regulation cannot actively suppress the temperature modulation
9 induced by the PTC, we needed to find another way to attenuate or even remove it. The
10 approach used was to add an extra, *active* heat oscillation source to the flange to
11 counterbalance the unwanted thermal oscillation. To test this idea theoretically, a sinusoidal
12 heat source was added onto the previous PI simulation model (figure 9). Because by definition
13 a heater cannot cool, the amplitude of this active sinusoidal heat must be lower than the heat
14 used in the previous PI regulation (in this case around 110 mW).

1 Theoretically, the addition of two sine-waves can either increase or decrease the total
2 amplitude. Thus, there exists an optimal phase relationship between this active sinusoidal heat
3 and the oscillation heating from PTC which makes the oscillation on the flange lowest. For
4 this reason, several phase angles from 0 to 2π were tested (amplitude set to 100 mW).
5 Figure 10 shows the simulation results. One sees as expected that the original temperature
6 oscillation can be either increased or decreased depending on the phase angle. For a phase
7 angle between $3\pi/4$ and π , the amplitude of the original oscillation is reduced to 1.4 mK. In
8 other words, the amplitude of the original temperature oscillation on the flange (2.75 mK) was
9 suppressed almost two-fold.

10 **5. Conclusion**

11 To understand PI regulation with temperature oscillation in a cryogen-free cryostat at
12 low temperature (5 K) cooled by a pulse-tube cooler, a simulation model was developed based
13 on the transfer-function method by using both the step response characteristic and the intrinsic
14 oscillation characteristic of cryostat. The results showed that the thermal response
15 characteristics of the cryostat can be well described by four transfer functions. They also
16 showed that the PI parameters mainly affect the overshoot value and stabilization time during
17 the regulation but have a negligible effect on the thermal oscillation amplitude. In other
18 words, the temperature oscillation cannot be suppressed using PI feedback alone. Based on
19 this observation, a new active suppression method was proposed and tested numerically.
20 According to calculations, it should reduce the original modulation amplitude by a factor of
21 two. The successful experimental implementation of the method will be described in a
22 companion paper submitted to this journal [25].

23 **Acknowledgments**

24 This work was supported by the National Key R&D Program of China (Grant No.
25 2016YFE0204200), the National Natural Science Foundation of China (Grant No. 51627809),
26 the International Partnership Program of the Chinese Academy of Sciences (Grant No.
27 1A1111KYSB20160017) and the European Metrology Research Programme (EMRP) project
28 : Real-K (No. 18SIB02). Changzhao Pan was supported by funding provided by an H2020
29 Marie Skłodowska Curie Individual Fellowship-2018 (834024).

30 **References**

- 1 1. Steur P P M, Durieux M. Constant-volume gas thermometry between 4 K and 100 K.
2 Metrologia, 1986, 23(1): 1 – 18
- 3 2. Gaiser C, Zandt T, Fellmuth B. Dielectric-constant gas thermometry. Metrologia,
4 2015, 52(5): S217-S226.
- 5 3. Pitre L, Moldover M R, Tew W L. Acoustic thermometry: new results from 273 K to
6 77 K and progress towards 4 K. Metrologia, 2006, 43(1): 142.
- 7 4. Gao B, Pitre L, Luo E C, et al. Feasibility of primary thermometry using refractive
8 index measurements at a single pressure. Measurement, 2017, 103: 258-262.
- 9 5. Verdier M A, Di Stefano P C F, Bonte F, et al. A 2.8 K cryogen-free cryostat with
10 compact optical geometry for multiple photon counting. Rev. Sci. Instrum., 2009, 80(4):
11 046105.
- 12 6. Chapman C R, Evans B E, Dudman M P, et al. Cryogen-free cryostat for neutron
13 scattering sample environment. Cryogenics, 2011, 51(3): 146-149.
- 14 7. Nakano T, Tamura O, Sakurai H. Comparison system for the calibration of capsule-
15 type standard platinum resistance thermometers at NMIJ/AIST. Int. J Thermophys., 2008,
16 29(3): 881-889.
- 17 8. Li R, Onishi A, Satoh T, et al. Temperature Stabilization on Cold Stage of 4 K GM
18 Cryocooler in Cryocoolers 9, Ronald G. Ross Jr., editor, Plenum Press, NY, 1997: 765-
19 771.
- 20 9. Okidono K, Oota T, Kurihara H, et al. Temperature oscillation suppression of GM
21 cryocooler, J. Phys.: Conference Series. IOP Publishing, 2012, 400(5): 052026.
- 22 10. Webber R J, Delmas J. Cool-down acceleration of GM cryocoolers with thermal
23 oscillations passively damped by helium, IOP Conference Series: Materials Science and
24 Engineering. IOP Publishing, 2015, 101(1): 012137.
- 25 11. Fluhr C, Dubois B, Grop S, et al. A low power cryocooled autonomous ultra-stable
26 oscillator. Cryogenics, 2016, 80: 164-173.
- 27 12. Huang Y, Weng J, Liu J. Experimental investigation on sub-miliKelvin temperature
28 control at liquid hydrogen temperatures. Cryogenics, 2014, 61: 158-163.
- 29 13. Allweins K, Qiu L M, Thummes G. Damping of intrinsic temperature oscillations in a
30 4 K pulse tube cooler by means of rare earth plates, AIP Conference Proceedings. 2008,
31 985(1): 109-116.
- 32 14. Shen X F, You L X, Chen S J, et al. Performance of superconducting nanowire single
33 photon detection system with different temperature variation. Cryogenics, 2010, 50(10):
34 708-710.

- 1 15. Nakamura D, Hasegawa Y, Murata M, et al. Reduction of temperature fluctuation
2 within low temperature region using a cryocooler. *Rev. Sci. Instrum.*, 2011, 82(4):
3 044903.
- 4 16. Dong B, Zhou G, Liu L Q, et al. A new cryostat for precise temperature control, AIP
5 Conference Proceedings. 2013, 1552(1): 825-829.
- 6 17. Dubuis G, He X, Božović I. Sub-millikelvin stabilization of a closed cycle cryocooler.
7 *Rev. Sci. Instrum.*, 2014, 85(10): 103902.
- 8 18. Gao B, Pan C, Pitre L, et al. Chinese SPRIGT realizes high temperature stability in the
9 range of 5–25 K. *Science Bulletin*, 2018, 63(12): 733-734.
- 10 19. Gao B, Pan C Z, Chen Y Y, et al. Realization of an ultra-high precision temperature
11 control in a cryogen-free cryostat. *Rev. Sci. Instrum.*, 2018, 89(10): 104901.
- 12 20. Chen Y Y, Zhang H Y, Song Y N, et al. Thermal response characteristics of a SPRIGT
13 primary thermometry system. *Cryogenics*, 2019, 97: 1-6.
- 14 21. Liu J, Sergatskov D A, Duncan R V. Adaptive optimal PI controller for high-precision
15 low-temperature experiments, Proceedings of the 2005, American Control Conference,
16 June 8-10, 2005. Portland, OR, US. IEEE, 2005: 4220-4224.
- 17 22. Li J, Lockhart J M, Boretsky P. Cryogenic precision digital temperature control with
18 peaked frequency response. *Rev. Sci. Instrum.*, 2004, 75(5): 1182-1187.
- 19 23. Bhatt, J.H., Dave, S.J. Mehta, M.M. Upadhyay, N. INROADS-An International
20 Journal of Jaipur National University, 5(1s), 336-340 (2016)
- 21 24. Sosso A, Durandetto P. Experimental analysis of the thermal behavior of a GM
22 cryocooler based on linear system theory. *Int. J. Refrig.*, 2018, 92: 125-132.
- 23 25. Pan C, Hu J, Zhang H, Song Y, et al. Active suppression of temperature oscillation
24 from a pulse tube cryocooler in a cryogen-free cryostat: Part 2. Experimental realization.
25 Submitted to *Cryogenics*.